

1 **Why some countries but not others? Urbanisation, GDP and endemic disease predict**  
2 **global SARS-CoV-2 excess mortality patterns.**

3

4 **Authors:** Nicholas M. Fountain-Jones<sup>1\*</sup>, Michael Charleston<sup>1</sup>, Emily Flies<sup>1,2</sup>, Scott Carver<sup>1</sup> &  
5 Luke Yates<sup>1</sup>

6 **Affiliations:**

7 <sup>1</sup> School of Natural Sciences, University of Tasmania, Hobart Australia 7001.

8 <sup>2</sup> Healthy Landscapes Research Group, University of Tasmania, Hobart Australia 7001

9

10 [\\*Nick.FountainJones@utas.edu.au](mailto:*Nick.FountainJones@utas.edu.au)

11

12 **Abstract**

13 The global impact of the SARS-CoV-2 pandemic has been uneven, with some regions  
14 experiencing significant excess mortality while others have been relatively unaffected. Yet  
15 factors which predict this variation remain enigmatic, particularly at large spatial scales. We  
16 used spatially explicit Bayesian models that integrate socio-demographic and endemic  
17 disease data at the country level to provide robust global estimates of excess SARS-CoV-2  
18 mortality (P scores) for the years 2020 and 2021. We find that gross domestic product (GDP),  
19 spatial patterns and urbanization are strong predictors of excess mortality, with countries  
20 characterized by low GDP but high urbanization experiencing the highest levels of excess  
21 mortality. Intriguingly, we also observed that the prevalence of malaria and human  
22 immunodeficiency virus (HIV) are associated with country-level SARS-CoV-2 excess  
23 mortality in Africa and the Western Pacific, whereby countries with low HIV prevalence but  
24 high malaria prevalence tend to have lower levels of excess mortality. While these  
25 associations are correlative in nature at the macro-scale, they emphasize that patterns of  
26 endemic disease and socio-demographic factors are needed to understand the global  
27 dynamics of SARS-CoV-2.

28 **Key words:** COVID-19, human immunodeficiency virus (HV), malaria, macroecology,  
29 spatial model

30

## 31 **Introduction**

32 Since the emergence of the SARS-CoV-2 pandemic in December 2019, there has been  
33 substantial interest in understanding the determinants of disease patterns and accurately  
34 assessing the true impact of this worldwide disaster. There have been a wide variety of  
35 approaches to estimating the mortality associated with SARS-CoV-2, but in each case,  
36 estimates of the true death toll have likely been orders of magnitude higher than reported  
37 deaths. Excess mortality, the difference in deaths due to a crisis compared to those expected  
38 under normal conditions [1], provides a more reliable estimate of COVID-19 deaths than  
39 reported deaths [2]. However, the factors shaping the heterogeneity of estimates of excess  
40 deaths across countries remain obscure.

41 Global estimates for the first epidemic waves in 2020/2021 range from 14.8 [2] to 18.2  
42 million excess deaths [3], dwarfing the 5.94 million reported deaths for the same period. For  
43 example, the World Health Organization (WHO) estimated Indonesia to have 1.03 million  
44 excess deaths up until December 2021 (credible interval (CI) 0.75-1.29 million) whereas 0.23  
45 million excess deaths were estimated in Pakistan (CI 0.04-0.4 million) [2], even though the  
46 population sizes of these countries are comparable. Africa has experienced much lower  
47 excess mortality compared to most other regions [2–5]. Deficiencies in the input data in  
48 developing countries may underly some of this variation, but these estimates are congruent  
49 with cross-sectional studies and reports [e.g., 6].

50 Comparing excess mortality estimates across countries is a challenging task as raw estimates  
51 are strongly dependent on population size and age structure of each country [2,7]. For  
52 example, larger populations with higher proportions of older people will have higher number  
53 of expected deaths compared to countries with smaller younger populations. To facilitate  
54 cross-country comparisons, estimates of excess deaths are often normalized by the expected

55 number of deaths (from all causes) across a period of time. The measurement of excess  
56 deaths, referred to as a P-score [7], takes into account both the population size and age  
57 structure (see *Methods*). For instance, if 100 deaths were anticipated but the actual number  
58 reached 150, resulting in 50 excess deaths, the P-score would be calculated as 50% [7]. Put  
59 another way, if a country had a P-score of 50% for a year then the reported death count was  
60 50% higher than the expected death count that year. Recent (as of February 2023) P-score  
61 estimates from the WHO have provided important insights into the relative toll of the  
62 pandemic across countries, with smaller countries in the Americas suffering relatively more  
63 excess deaths (highest P-scores), even though they experienced fewer absolute deaths  
64 compared to larger countries [2]. For example, Peru had an estimated P-score of 97% or  
65 effectively a doubling of deaths during the first waves of the pandemic [2]. Other countries,  
66 such as Australia where infection rates were low were estimated to have negative values as  
67 there were actually fewer deaths during these years than expected [2].

68 Clearly, differences in pandemic response explain some variation in global P-Score estimates  
69 but these are not sufficient to explain the general patterns [2]. Here we build a fully  
70 probabilistic model accounting for uncertainties in P-score estimates to test if socio-  
71 demographic, economic and patterns of endemic disease could help predict these disparate  
72 estimates of excess mortality across countries. While P-scores control for age structure of a  
73 population, age is a well-known risk factor for mortality, some countries with larger portions  
74 of the population > 70 y.o. are likely to experience higher mortality than countries with fewer  
75 people in this age bracket [e.g., 8]. As P-scores capture direct and indirect SARS-CoV-2  
76 deaths (e.g., because patients could not access treatment that would be otherwise available),  
77 the prevalence of non-communicable conditions such as heart disease [9] may also play a role  
78 in shaping these excess deaths. Economic variables such as gross domestic product (GDP)  
79 [30] and health spending may also impact mortality rates as countries with high GDP and

80 health spending may lower mortality risks through, for example, better treatment. Countries  
81 with high population density and urbanisation may also experience higher mortality as  
82 transmission may be facilitated in these conditions [10] or lower, because urban populations  
83 tend to have better access to health facilities [11]. Further, our previous work has also found  
84 that variation in the prevalence of endemic pathogens including malaria (*Plasmodium* sp.),  
85 common intestinal parasitic worms (e.g., *Trichuris trichiura*, the causative agent of  
86 ascariasis) and human immunodeficiency virus (HIV) played a surprisingly important role in  
87 predicting variation in SARS-CoV-2 reported deaths [12]. For example, countries with  
88 relatively high prevalence of endemic malaria had reduced numbers of deaths, whereas  
89 countries with higher HIV prevalence had higher numbers of reported deaths (while  
90 controlling for other factors such as the mean age of the country) [12].

91 Spatial relationships are also likely to be important in explaining variation in P-scores and  
92 need to be accounted for in global models [e.g., 13]. For example, regions or countries closer  
93 in space may have similar P-scores due to similar epidemic trajectories [14]. High  
94 connectivity between neighbouring countries could also facilitate the spread of the virus and  
95 increase mortality. International air travel is also known to facilitate SARS-CoV-2 spread  
96 among countries [13,15,16], and countries with high air travel connectivity with other  
97 countries may have increased numbers of introduction events which may result in higher  
98 mortality. Countries with high connectivity also tended to have the earliest outbreaks of the  
99 virus [17].

100 In this study, we introduce a Bayesian model-based framework with the aim to discover the  
101 potential drivers behind the variations in excess deaths across countries. By utilizing this  
102 model-based approach, we illuminate factors that contribute to the diverse severity of the  
103 pandemic's consequences worldwide.

## 104 **Methods**

### 105 *Data retrieval*

106 We extracted P-score estimates from the WHO excess mortality code base on the 3<sup>rd</sup> of  
107 March 2023 (the <https://github.com/WHOexcessc19/Codebase>). We computed the posterior  
108 mean and its standard error for the average P-score estimates across the 24 months spanning  
109 2020 and 2021. We used only data for the first wave of SARS-CoV-2 to examine infection  
110 patterns without the influence of the variable roll-out of vaccines. We also used the WHO  
111 transmission classification scheme (i.e., countries with community transmission, clusters of  
112 cases only, sporadic cases and no cases) to account for differences in pandemic response (as  
113 of 29<sup>th</sup> of January 2021, the midpoint of our excess mortality estimates).

114 We leveraged the predictor variables collated previously [see 12 for further details]. Briefly,  
115 we extracted demographic and economic variables from the World Bank dataset  
116 (<https://data.worldbank.org/>) for each country. These variables include per capita GDP (in  
117 current USD averaged across 2014-2019), percent of the population living in urban areas  
118 (hereafter percent urban). Global health spending estimates (USD) are calculated by the  
119 World Health Organization and include healthcare goods and services consumed each year.  
120 To analyse the importance of spatial patterns to P-score estimates we constructed a lagged P-  
121 score variable based on a neighbourhood matrix. To construct the neighbourhood matrix, we  
122 extracted centroid coordinates of countries and generated spatial neighbourhood matrix based  
123 on the mean P-score estimate using the *spdep* package in R [18]. To capture the role of  
124 country-level connectivity in predicting P-scores, we incorporated the 2007 air connectivity  
125 index [16]. We attempted to include an intrinsic spatial conditional autoregressive (iCAR)  
126 term to our model, yet we could not attain model convergence with this extra complexity.

127 We downloaded the mean estimate of prevalence of 14 endemic diseases in each country  
128 (Table S1) based on 2019 data from the Institute for Health Metrics and Evaluation (IHME)  
129 Global Burden of Disease (GBD) database ([https://www.healthdata.org/research-](https://www.healthdata.org/research-analysis/gbd)  
130 [analysis/gbd](https://www.healthdata.org/research-analysis/gbd)). As many of the country-level disease prevalence estimates were correlated, we  
131 conducted principal component analysis (PCA) and we used the top three resultant  
132 orthogonal principal components as predictors in our models. As malaria and HIV were not  
133 correlated with any of the principal components, we included these variables separately. To  
134 measure overall infectious disease burden, we also extracted estimates of years of life lost  
135 (YLLs) for infectious diseases combined in each country in 2019 using the GBD data. We  
136 extracted diabetes prevalence and the average cardiovascular death rate for each country in  
137 2019 from the GBD also. See Table S1 for a complete list of predictors used.

138 We imputed missing data for both datasets dataset using classification and regression trees as  
139 implemented in the multivariate imputation by chained equations (MICE) package [19]. We  
140 generated ten separate multiple imputations and combined the posterior distributions across  
141 the ten corresponding model fits to marginalise over the uncertainty of the replacement  
142 values. We screened variables for collinearity by calculating Pearson's correlation  
143 coefficient ( $\rho$ ) and for correlated pairs excluded the variable with the highest correlation  
144 across the complete dataset.

#### 145 *Bayesian modelling*

146 We modelled P-score variation globally using generalised additive models (GAM) with a  
147 Gaussian error distribution to facilitate the inclusion of response errors (i.e., the uncertainty  
148 of the P-score estimates) and since the P-scores values are naturally unconstrained. The  
149 advantage of GAMs over linear models is their flexibility to capture a wide range of non-  
150 linear functional forms using splines while mitigating overfitting through smoothing (we set

151 the maximal basis dimensions of the splines to 6 to flexibly capture non-linear relationships  
152 while keeping the effective model complexity under control). Specifically, our models  
153 quantified the probability of observing P-scores ( $y_i$ ) in country  $i$  given by:

$$p(y_i | \mu_i, \sigma_i, se_i) = N(\mu_i, \sigma_i^2 + se_i^2)$$

154 where  $se_i = se(y_i)$  is the standard error of the response and  $\mu_i$  and  $\sigma_i^2$  are the modelled mean  
155 and variance, respectively. Models for each of the distributional parameters are given by:

$$\mu_i = \beta_0 + b_{\text{region}[i]} + \beta_{\text{trans}[i]} + \sum_k^p f_k(X_{ki}) \quad (2)$$

$$\log \sigma_i = \alpha_0 + a_{\text{region}[i]} \quad (3)$$

156 where  $\alpha_0$  and  $\beta_0$  are global intercepts,  $a$  and  $b$  are region-level (random) intercepts,  $\beta_{\text{trans}}$  is a  
157 fixed effect for transmission type,  $p$  number of predictors included in the model and  $f_k(X_{ki})$   
158 are smooth spline terms for each continuous predictor  $X_k$ . The region-level intercepts  
159 ( $a_{\text{region}[i]}$ ,  $b_{\text{region}[i]}$ ) were drawn from a bivariate normal distribution with an estimated  
160 three-parameter covariance matrix. The basis elements for each thin plate smoothing spline  
161 were generated using the R package *mgcv* [20] and the corresponding regression coefficients  
162 were drawn from a normal distribution parametrised by an estimated smoothing  
163 hyperparameter.

164 All models were fit in a Bayesian framework using Hamiltonian Monte Carlo (HMC)  
165 methods [21] and ‘no U-turn sampling’ (NUTS, [22]), as implemented in the R package  
166 ‘*brms*’ [23]. We ran four chains of 12000 iterations, using weakly informative priors---the  
167 prior for the smoothing hyperparameter was half student-t distribution (df = 3, scale = 2.6),  
168 and inferences proved robust to changes in the choice of scale. To establish chain  
169 convergence, we used the rank-normalised  $\hat{R}$  statistic ( $\hat{R} < 1.01$ ) [24] as well as visual



170 inspection. We validated the model by comparing pointwise posterior-predictive intervals to  
171 the observed P-scores for each country [25].

172 To interrogate our model, we computed conditional effects for each covariate. For the  
173 numeric variables, we computed the estimated change in response (centred on the posterior-  
174 predictive mean) as a function of changes in the value of a given predictor (centred on the  
175 global mean) while holding all other variables at their global means. Variables were  
176 considered strong predictors of P-scores if the 90% credible interval (CI) did not include 0.  
177 Variables where this was true for a smaller portion of the range were identified as weaker  
178 variables (variables where all values of the CI included 0). To test the utility of adding  
179 endemic disease variables to our macroecological models, we evaluated model performance  
180 using approximate leave-one-out cross validation (LOO, [26]) an estimate of relative  
181 expected Kullback–Leibler discrepancy and compared the model both with and without the  
182 inclusion of endemic pathogens. We also compared model performance by region. Our  
183 complete workflow and data are available on github:  
184 ([https://github.com/nfj1380/covid19\\_macroecology](https://github.com/nfj1380/covid19_macroecology)).

185

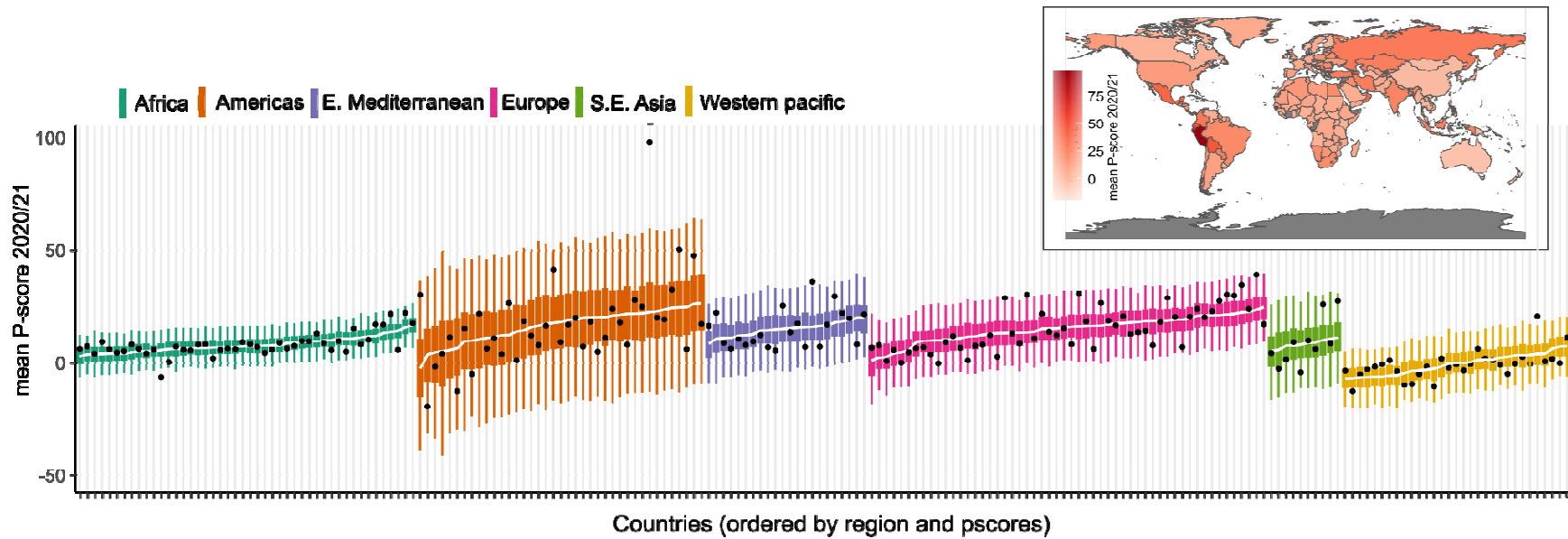
## 186 **Results**

187

188 Our model was able to predict global P-score variation remarkably well with mean observed  
189 P-scores from 175 out of 181 countries inside the model credible intervals (Fig. 1). Our  
190 model underestimated excess mortality for five countries and only overestimated P-scores  
191 from Togo. Our model could not predict the P-score for Peru (the highest mean P-score  
192 calculated, Fig. 1 inset) but our predictive performance was high for countries with very low  
193 or negative P-scores. Our models also underestimated excess mortality in Guam, Oman,

194 Andorra and Armenia (Fig. S1). There was overall no difference in model performance  
195 across regions, but countries in the Americas had much higher uncertainty in P-score  
196 estimates compared to the other regions. (Fig. 1).

197



198

199 **Fig. 1:** Posterior predictive performance of our P-score model for each country and (inset) the global distribution of mean P-scores across  
200 countries. Countries are grouped by region and ordered by predicted values (lowest to highest). Black dots are the observed values for each  
201 country and the trend line is the median posterior estimate of the models. Credible intervals (CIs) are coloured by region, with the 50% and 95%  
202 CIs depicted by thick and thin lines, respectively. See Fig. S1 for predictions with each country labelled.

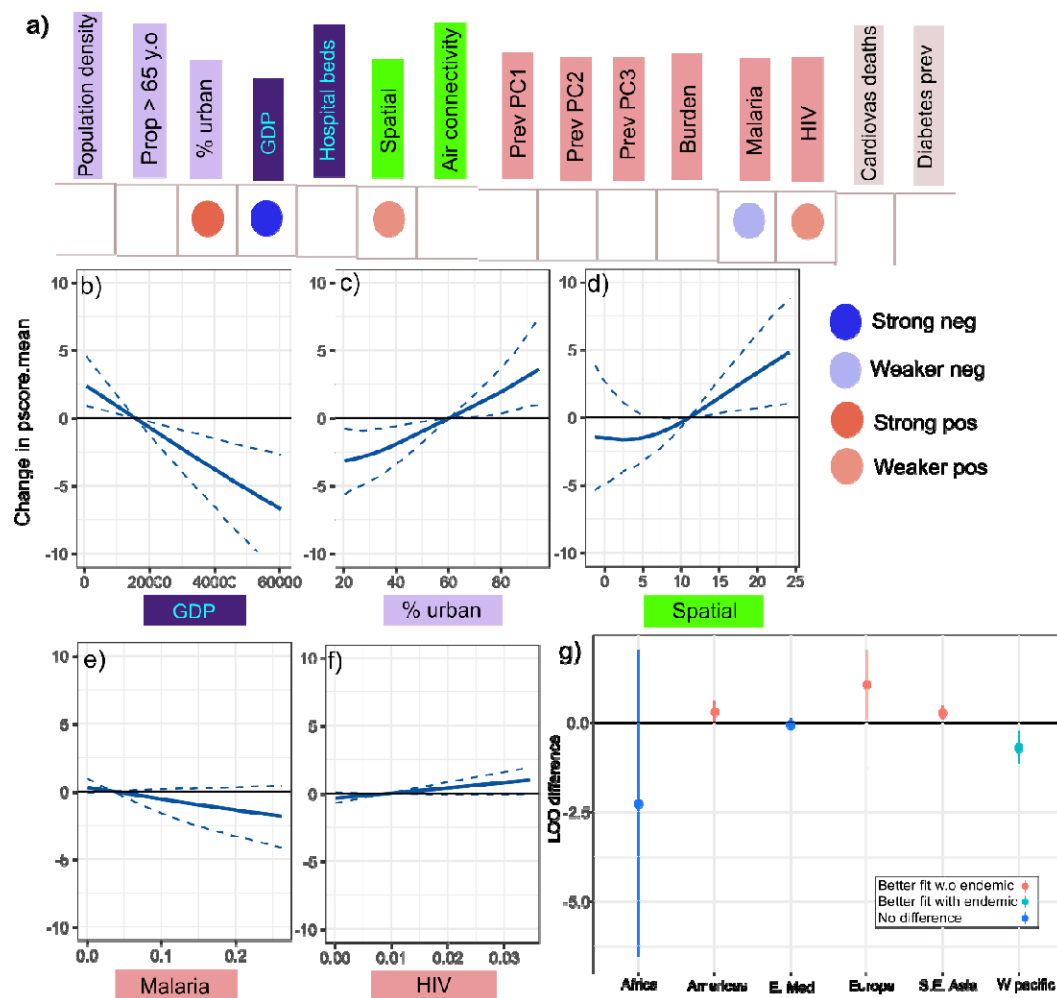
203 We found a mix of population, spatial patterns and endemic disease that best predicted P-  
204 score variation in our models (Fig. 2). Though important at individual or within country  
205 scales, variables such as proportion over 65 y.o., population density and air-connectivity were  
206 less important at global scales (Fig. 2a). We also did not see a signature of diabetes  
207 prevalence or cardiovascular disease impacting P-score estimates (Fig. 2a, see Fig S2 for the  
208 conditional effects plots).

209 Per-capita GDP and percent urban were strong predictors of P-score variation (Fig. 2a/b).  
210 Wealthier countries with a per-capita GDP >\$20,000 had decreased P-scores (while  
211 controlling for all other predictors in the model, Fig. 2b). GDP decreased excess mortality by  
212 up to 10% in countries with a GDP of ~\$60,000 (e.g., USA, Iceland, and Singapore).  
213 Conversely, countries with >60% urban population had higher P-scores (Fig. 2b). Spatial  
214 patterns played a role and the effect was non-linear (Fig. 2a/b). Countries with neighbours  
215 having average P-scores >12 also exhibited higher P-scores (Fig. 2b).

216 We also detected divergent (but weaker) relationships with malaria and HIV prevalence on P-  
217 scores (Fig. 2a). While holding all other variables in the model at their mean value, countries  
218 with relatively high prevalence of malaria had decreased P-scores, whereas countries with  
219 relatively high HIV prevalence had higher P-scores. The estimated LOO scores indicated that  
220 retaining endemic disease variables in the model did not improve model fit overall (ELPD  
221 difference = - 1.4, SE = 4.4), although including endemic disease did improve predictions in  
222 the Western Pacific (Fig. 2c). There was also some evidence that the fit was improved by  
223 endemic disease in Africa but the LOO scores were highly variable which could indicate that  
224 we are missing important variables in this region. For Europe and the Americas in contrast,  
225 model fit was improved by not including the endemic disease variables (i.e., LOO model

226 difference scores above 0). Collectively, there appears some regional scale context-dependent  
227 relationships between SARS-CoV-2 P-scores and endemic disease.

228



229

230 **Fig 2:** Conditional effects of model predictors on the expected change in global P-scores. a) and direction of covariate effects on P-scores. Pos = positive, Neg = negative. Covariates  
 231 without a corresponding circle (i.e., blank) had little impact on P-score estimates (see Fig.  
 232 S2). b-f) Conditional plots showing the expected difference in P-scores as a function of the  
 233 difference between a given covariate value and the mean observed covariate values (CIs have a  
 234 width of 0 at the mean, see *Methods*). span the predictors included in the model. Solid lines  
 235 denote the posterior means and the associated intervals (dashed lines) denote the 90%  
 236 credible intervals (CIs). Predictors are colour-coded based on variable type (dark blue =  
 237 associated with a country's economic capacity, light red = country level pathogen prevalence  
 238 estimate, light grey = estimated prevalence of non-infectious disease, light green = spatial  
 239 variable, purple = population characteristic. Spatial: estimates of cases in neighbouring  
 240 countries. HIV: Human immunodeficiency virus. (see Table S1 for details). g) Leave one out  
 241 (LOO) comparisons of our model with all co-variates compared to a model leaving out the  
 242 endemic disease variables summed across regions. Region level estimates not overlapping the  
 243 0 LOO difference were considered significant. W.o = without.

245

246 **Discussion**

247

248 Our study provides some important insights into the divergent impacts of the SARS-CoV-2  
249 pandemic. Our Bayesian analytical approach combined with robust estimates of excess deaths  
250 from the WHO revealed that GDP, urbanisation and spatial patterns played an important role  
251 in predicting excess mortality across countries. We also found that malaria and HIV were  
252 associated with excess deaths, particularly in the Western Pacific and African regions, but not  
253 necessarily in other regions of the world. Studies at this scale, while necessarily associative,  
254 can help identify plausible drivers of variation in SARS-CoV-2 mortality at large spatial  
255 scales.

256

257 We identified that highly urban countries with low GDP and surrounded by countries with  
258 high P-Scores had the highest levels of excess mortality during the first waves of the  
259 pandemic. Endemic disease patterns also had some association, but comorbidities such as  
260 diabetes prevalence and proportion of the population > 65 y.o. were less relevant at the scale  
261 of our analysis. The relationship between GDP and SARS-CoV-2 mortality has generally  
262 been found to be positively correlated with the number of reported deaths higher in countries  
263 with higher GDP [e.g., 27]. Our model using the more robust P-score estimates of excess  
264 mortality suggest the opposite trend; potentially as our estimates are less-impacted by  
265 reporting biases in countries with fewer resources. GDP is strongly correlated with health  
266 spending, so it is possible that the quality of health care afforded by countries with high GDP  
267 is associated with reduced excess mortality. However, even after accounting for GDP, the  
268 burden of excess mortality is not shared evenly. Highly urban populations are known to be  
269 vulnerable to SARS-CoV-2 mortality as urban areas are densely populated and are travel

270 hubs, both of which facilitate transmission [10,12,16,27]. Despite the benefits of living in  
271 cities, such as better access to medical resources, our study demonstrates that urban areas face  
272 amplified SARS-CoV-2-related mortality [11].

273

274 Highly urban countries are often more connected to other countries, yet higher air  
275 connectivity alone did not explain P-score variation in our model. Spatial relationships as  
276 well as regional variability were more important and similar results have been found in  
277 models focusing on global patterns of confirmed deaths [12]. In our analysis, a clear  
278 threshold emerged indicating a spatial effect, where mean P-scores increased when the  
279 average of neighbouring countries exceeded approximately 10. This finding suggests  
280 geographically constrained patterns, with countries experiencing high transmission and  
281 mortality influencing neighbouring P-scores through cross-border transmission.

282

283 We also provide further evidence for the effect of endemic pathogen prevalence on global  
284 SARS-CoV-2 mortality with countries with lower malaria prevalence but higher HIV  
285 prevalence tending to have higher P-scores. While the effect at a global level was marginal,  
286 our interrogation of regional level patterns found that endemic pathogens were associated  
287 with P-score patterns in the regions with high burdens of endemic disease. Our findings are  
288 similar to other studies modelling deaths at this scale and our previous work [12,16]. In these  
289 regions, coinfections with either of these pathogens and SARS-CoV-2 were common and  
290 coinfection can impact the severity of SARS-CoV-2 [28–30]. For example,  
291 immunocompromised HIV patients can face a higher risk of severe SARS-CoV-2 infection  
292 [31]. At a coarser scale, countries in Africa with high-levels of mortality also had the highest  
293 prevalence of HIV [16]. Additionally, there is evidence suggesting that malaria can influence



294 the mortality rates of SARS-CoV-2 by mitigating the severity of the illness [29,32]. For  
295 instance, a study conducted on healthcare workers in India revealed that individuals  
296 coinfecting with malaria and SARS-CoV-2 experienced an average recovery period that was  
297 eight days shorter than those who were infected with SARS-CoV-2 alone [29].

298

299 Though our model for the most part could predict country-level P-scores well, it is important  
300 to acknowledge that this was not the case for all countries. For example, the P-score for Peru  
301 exceeded our model estimates. Why Peru is globally unique is unclear, but may be linked to  
302 failures in the health system coupled with diverse populations with high levels of poverty  
303 [33]. Although we gathered a diverse range of predictors, the dataset is not comprehensive,  
304 and we may have missed important axes of variation. Our objective was to include as many  
305 countries as possible in the analysis while minimizing missing data. Our data was also  
306 aggregated at the country-level and we possibly missed important variation within countries  
307 that may provide high resolution predictions of SARS CoV-2 mortality. Moreover, while our  
308 model was able to propagate the estimated uncertainty with the WHO's modelled P-scores, it  
309 is important to recognise some features of WHO's generation of the P-scores themselves. The  
310 WHO found that tracking excess mortality directly in some parts of the world, particularly in  
311 sub-Saharan Africa, was not possible and within-country estimates relied on statistical  
312 models [2]. We urge caution when interpreting our cross-country models in the region. Still  
313 as reported deaths data are likely a severe undercount in sub-Saharan Africa [2,34], model-  
314 based P-score estimates provide the most reliable estimates of SARS-CoV-2 mortality in the  
315 region.

316

317 Our study highlights factors associated with variation in excess mortality across countries and  
318 provides insights into why some countries were impacted more by the pandemic than others.  
319 By understanding the predictors of P-score variation across countries and gaining insights  
320 into the differential impacts of the pandemic, we may be able to better inform global  
321 strategies for outbreak management and response. For example, our model estimates suggest  
322 that targeting medical resources to highly urban countries with low GDP and high HIV  
323 prevalence may reduce mortality during future outbreaks. Future investigations should aim to  
324 explore these global factors using increasingly accurate mortality estimates and consider the  
325 dynamics of new waves of SARS-CoV-2.

#### 326 **Data availability statement**

327 All data and code used to perform the analyses presented in this paper are available on  
328 Github: [https://github.com/nfj1380/covid19\\_macroecology](https://github.com/nfj1380/covid19_macroecology)

#### 329 **Acknowledgements**

330 This project was supported by an Australian Research Council Discovery Project Grant  
331 (DP190102020).

#### 332 **Conflicts of interest**

333 None to declare

334

## 335 **References**

- 336 1. Checchi F, Roberts L. In press. A primer for non-epidemiologists.
- 337 2. Msemburi W, Karlinsky A, Knutson V, Aleshin-Guendel S, Chatterji S, Wakefield J. 2023  
338 The WHO estimates of excess mortality associated with the COVID-19 pandemic.  
339 *Nature* **613**, 130–137. (doi:10.1038/s41586-022-05522-2)
- 340 3. Wang H *et al.* 2022 Estimating excess mortality due to the COVID-19 pandemic: a  
341 systematic analysis of COVID-19-related mortality, 2020–21. *The Lancet* **399**, 1513–  
342 1536. (doi:10.1016/S0140-6736(21)02796-3)
- 343 4. 2023 The pandemic's true death toll. *The Economist*. See  
344 <https://www.economist.com/graphic-detail/coronavirus-excess-deaths-estimates>  
345 (accessed on 24 May 2023).
- 346 5. Bouba Y, Tsinda EK, Fonkou MDM, Mmbando GS, Bragazzi NL, Kong JD. 2021 The  
347 Determinants of the Low COVID-19 Transmission and Mortality Rates in Africa: A Cross-  
348 Country Analysis. *Front Public Health* **9**, 751197. (doi:10.3389/fpubh.2021.751197)
- 349 6. Salyer SJ *et al.* 2021 The first and second waves of the COVID-19 pandemic in Africa: a  
350 cross-sectional study. *The Lancet* **397**, 1265–1275. (doi:10.1016/S0140-6736(21)00632-  
351 2)
- 352 7. In press. A pandemic primer on excess mortality statistics and their comparability across  
353 countries. *Our World in Data*. See <https://ourworldindata.org/covid-excess-mortality>  
354 (accessed on 24 May 2023).
- 355 8. Sorci G, Faivre B, Morand S. 2020 Explaining among-country variation in COVID-19  
356 case fatality rate. *Sci Rep* **10**, 18909. (doi:10.1038/s41598-020-75848-2)
- 357 9. Han L, Zhao S, Li S, Gu S, Deng X, Yang L, Ran J. 2023 Excess cardiovascular  
358 mortality across multiple COVID-19 waves in the United States from March 2020 to  
359 March 2022. *Nat Cardiovasc Res* **2**, 322–333. (doi:10.1038/s44161-023-00220-2)
- 360 10. González-Val R, Sanz-Gracia F. 2022 Urbanization and COVID-19 incidence: A cross-  
361 country investigation. *Papers in Regional Science* **101**, 399–415.  
362 (doi:10.1111/pirs.12647)
- 363 11. Scheil-Adlung X. 2015 Global evidence on inequities in rural health protection: new  
364 data on rural deficits in health coverage for 174 countries. *ILO Working Papers*
- 365 12. Fountain-Jones NM, Yates L, Flies E, Flies A, Carver S, Charleston M. 2021 Patterns of  
366 SARS-CoV-2 exposure and mortality suggest endemic infections, in addition to space  
367 and population factors, shape dynamics across countries. *medRxiv*,  
368 2021.07.12.21260394. (doi:10.1101/2021.07.12.21260394)
- 369 13. Krisztin T, Piribauer P, Wögerer M. 2020 The spatial econometrics of the coronavirus  
370 pandemic. *Lett Spat Resour Sci* **13**, 209–218. (doi:10.1007/s12076-020-00254-1)
- 371 14. Lacasa L, Challen R, Brooks-Pollock E, Danon L. 2020 A flexible method for optimising  
372 sharing of healthcare resources and demand in the context of the COVID-19 pandemic.  
373 *PLOS ONE* **15**, e0241027. (doi:10.1371/journal.pone.0241027)

- 374 15. Zhong L, Diagne M, Wang W, Gao J. 2021 Country distancing increase reveals the  
375 effectiveness of travel restrictions in stopping COVID-19 transmission. *Commun Phys* **4**,  
376 1–12. (doi:10.1038/s42005-021-00620-5)
- 377 16. Zhang F *et al.* 2021 Predictors of COVID-19 epidemics in countries of the World Health  
378 Organization African Region. *Nat Med* **27**, 2041–2047. (doi:10.1038/s41591-021-01491-  
379 7)
- 380 17. Bickley SJ, Chan HF, Skali A, Stadelmann D, Torgler B. 2021 How does globalization  
381 affect COVID-19 responses? *Globalization and Health* **17**, 57. (doi:10.1186/s12992-021-  
382 00677-5)
- 383 18. Bivand R, Piras G. 2015 Comparing Implementations of Estimation Methods for Spatial  
384 Econometrics. *Journal of Statistical Software* **63**, 1–36. (doi:10.18637/jss.v063.i18)
- 385 19. Azur MJ, Stuart EA, Frangakis C, Leaf PJ. 2011 Multiple imputation by chained  
386 equations: what is it and how does it work? *Int J Methods Psychiatr Res* **20**, 40–49.  
387 (doi:10.1002/mpr.329)
- 388 20. Wood S. In press. Generalized Additive Models: An Introduction with R, Second Edition -  
389 . See [https://www.routledge.com/Generalized-Additive-Models-An-Introduction-with-R-  
390 Second-Edition/Wood/p/book/9781498728331](https://www.routledge.com/Generalized-Additive-Models-An-Introduction-with-R-Second-Edition/Wood/p/book/9781498728331) (accessed on 8 July 2021).
- 391 21. Neal RM. 2011 MCMC using Hamiltonian dynamics. *arXiv:1206.1901 [physics, stat]*  
392 (doi:10.1201/b10905)
- 393 22. Homan MD, Gelman A. 2014 The No-U-turn sampler: adaptively setting path lengths in  
394 Hamiltonian Monte Carlo. *J. Mach. Learn. Res.* **15**, 1593–1623.
- 395 23. Bürkner P-C. 2017 brms: An R Package for Bayesian Multilevel Models Using Stan.  
396 *Journal of Statistical Software* **80**, 1–28. (doi:10.18637/jss.v080.i01)
- 397 24. Vehtari A, Gelman A, Simpson D, Carpenter B, Bürkner P-C. 2021 Rank-Normalization,  
398 Folding, and Localization: An Improved  $\hat{R}$  for Assessing Convergence of MCMC.  
399 *Bayesian Analysis* **1**, 1–38. (doi:10.1214/20-BA1221)
- 400 25. Gabry J, Simpson D, Vehtari A, Betancourt M, Gelman A. 2019 Visualization in Bayesian  
401 workflow. *Journal of the Royal Statistical Society: Series A (Statistics in Society)* **182**,  
402 389–402. (doi:10.1111/rssa.12378)
- 403 26. Vehtari A, Gelman A, Gabry J. 2017 Practical Bayesian model evaluation using leave-  
404 one-out cross-validation and WAIC. *Stat Comput* **27**, 1413–1432. (doi:10.1007/s11222-  
405 016-9696-4)
- 406 27. Skórka P, Grzywacz B, Moroń D, Lenda M. 2020 The macroecology of the COVID-19  
407 pandemic in the Anthropocene. *PLOS ONE* **15**, e0236856.  
408 (doi:10.1371/journal.pone.0236856)
- 409 28. Bradbury RS, Piedrafita D, Greenhill A, Mahanty S. 2020 Will helminth co-infection  
410 modulate COVID-19 severity in endemic regions? *Nat Rev Immunol* **20**, 342.  
411 (doi:10.1038/s41577-020-0330-5)
- 412 29. Mahajan NN *et al.* 2021 Co-infection of malaria and early clearance of SARS-CoV-2 in  
413 healthcare workers. *Journal of Medical Virology* **93**, 2431–2438.  
414 (doi:https://doi.org/10.1002/jmv.26760)

- 415 30. Miguel DC, Brioschi MBC, Rosa LB, Minori K, Grazzia N. 2021 The impact of COVID-19  
416 on neglected parasitic diseases: what to expect? *Trends in Parasitology* **37**, 694–697.  
417 (doi:10.1016/j.pt.2021.05.003)
- 418 31. Huang J *et al.* 2020 Epidemiological, virological and serological features of COVID-19  
419 cases in people living with HIV in Wuhan City: A population-based cohort study. *Clin*  
420 *Infect Dis* , ciaa1186. (doi:10.1093/cid/ciaa1186)
- 421 32. Achan J *et al.* 2022 Current malaria infection, previous malaria exposure, and clinical  
422 profiles and outcomes of COVID-19 in a setting of high malaria transmission: an  
423 exploratory cohort study in Uganda. *The Lancet Microbe* **3**, e62–e71.  
424 (doi:10.1016/S2666-5247(21)00240-8)
- 425 33. Taylor L. 2021 Covid-19: Why Peru suffers from one of the highest excess death rates in  
426 the world. *BMJ* **372**, n611. (doi:10.1136/bmj.n611)
- 427 34. Cabore JW *et al.* 2022 COVID-19 in the 47 countries of the WHO African region: a  
428 modelling analysis of past trends and future patterns. *The Lancet Global Health* **10**,  
429 e1099–e1114. (doi:10.1016/S2214-109X(22)00233-9)
- 430  
431